surfaces

MDPI

Article

Microplastic-Related Leachate from Recycled Rubber Tiles: The Role of TiO_2 Protective Coating

Paula Benjak [1], Lucija Radetić [1,*], Ivana Presečki [1,*], Ivan Brnardić [2], Nikola Sakač [1] and Ivana Grčić [1]

[1] Faculty of Geotechnical Engineering, University of Zagreb, Hallerova aleja 7, HR-42000 Varaždin, Croatia; pbenjak@gfv.hr (P.B.); nsakac@gfv.hr (N.S.); igrcic@gfv.hr (I.G.)
[2] Faculty of Metallurgy, University of Zagreb, Aleja narodnih heroja 3, HR-44000 Sisak, Croatia; brnardic@simet.unizg.hr
* Correspondence: lradetic@gfv.hr (L.R.); ivana.presecki@gfv.hr (I.P.)

Abstract: The extensive global use of rubber results in significant microplastic pollution from the release of tire wear particles and microplastic leachate, impacting the environment, human health, and ecosystems. Waste tires are normally recycled and used for the production of new products, such as rubber tiles. The presented study aims to show the possibility of further decrease in the negative environmental impact of materials based on recycled rubber. This paper presents the modification of rubber tiles with a titanium dioxide (TiO_2) coating, focusing on surface integrity, rubber particle wear release, and the consequent environmental impact of leachate release. Both reference and modified rubber tiles were subjected to artificial accelerated aging in a solar simulator for 4, 6, and 8 weeks, followed by an abrasion test. The carbonyl index was calculated from FTIR characterization after each time frame to indicate the degradation of organic compounds and chemical changes caused by UV exposure. A 24 h leaching test with a liquid-to-sample ratio of 1:20 was performed on both rubber tile samples prior to and after 8 weeks of aging along with the aged wear particles for the purpose of the non-target screening of released organic leachate by LC/MS QTOF. The results of carbonyl indices showed that the TiO_2 coating contributes to the stabilization of polymer degradation and, to a certain extent, reduces the leaching of organic compounds, such as phthalates. However, the increased wear and release of rubber particles and the subsequent degradation of organic leachates require further in-depth research.

Keywords: waste tires; rubber tiles; titanium dioxide; surface aging; microplastics leachate

Citation: Benjak, P.; Radetić, L.; Presečki, I.; Brnardić, I.; Sakač, N.; Grčić, I. Microplastic-Related Leachate from Recycled Rubber Tiles: The Role of TiO_2 Protective Coating. *Surfaces* **2024**, *7*, 786–800. https://doi.org/10.3390/surfaces7030051

Academic Editor: Gaetano Granozzi

Received: 30 June 2024
Revised: 12 September 2024
Accepted: 16 September 2024
Published: 18 September 2024

1. Introduction

Rubber is ubiquitous in everyday life; it is vital to our lives and difficult to replace. Many people are unaware of our reliance on this material and the fact that our current way of life would likely be impossible without it [1]. One of the most important revolutions involving rubber was the development of automobile tires, which made widespread travel possible [1,2]. In 2020, new-tire sales in Europe accounted for 324 million units, 89.5% (70 wt%) for passenger cars and light duty vehicles, 4.9% (20 wt%) for heavy duty vehicles (trucks and buses), 3.6% (1 wt%) for motorbikes and scooters, and 1.9% (9 wt%) for agricultural and off-road vehicles [1,2]. The automotive sector accounted for 65% of general tire production. The rubber can withstand both heat and cold and is resistant to a number of chemicals. There is a continuous search for new substances, compounds, and materials to improve the performance of final rubber products and replace them with safer and cheaper alternatives [1]. Despite all the benefits of rubber, it has a high environmental impact, since it is not biodegradable [3]. Rubber degrades over time due to environmental factors such as heat, light, and ozone, which cause molecular changes that can significantly affect its mechanical properties and service life [4]. It is well known that tires degrade when exposed to light, particularly ultraviolet (UV) irradiation, making it essential to study and understand this degradation as the use of rubber in outdoor applications increases [5,6].

Alongside rubber, plastic is also one of the most widely used materials today [7,8] due to its corrosion resistance, light fastness, and low cost [9,10]. However, widespread use has led to significant environmental pollution [8,11–13]. At first, concerns centered on the biodegradability of synthetic polymers from aspects of waste management. Later, the focus shifted to the release of microplastic particles (MPs), defined as fragments smaller than 5 mm, according to the US National Oceanic and Atmospheric Administration (NOAA), the European Chemicals Agency, and the United Nations Environment Program (UNEP) [8,9]. This caused significant concern about the potential adverse impact on human health and ecosystem [8,10,12–15]. Microplastics are categorized as being primary, created during manufacturing, and secondary, created from the breakdown of larger plastic due to mechanical stress, hydrolysis, oxidation, UV exposure, heat, and microorganisms [16], with secondary microplastics being the main contributor to the total amount of microplastic pollution [17]. Furthermore, tire tread wear particles are one of the major sources of microplastics, dispersing into water, air, and soil [18–26]. These particles are formed either by tire abrasion from traffic, known as tire and road wear particles (TRWPs) [23], from recycled tire crumbs, or from particles generated during tire repairs. They are collectively referred to as tire wear microplastics (TWMs) [15,27,28]. Annually, approximately 6,000,000 tons of TWMs are released into the environment worldwide [15,21,22,29–32]. Apart from microplastics, various chemicals used as additives in rubber are not covalently linked, allowing harmful substances like PAHs, heavy metals, and zinc to leach into the environment, posing risks to human health and aquatic organisms by acting as carcinogens, endocrine disruptors, and mutagens with bioaccumulation and toxicity potential [33,34]. Monitoring rubber particles is challenging and requires standardized methods to accurately assess their presence and impact [35–37]. Non-targeted analysis has provided deeper insights into the complex chemical mixtures that can leach from tire materials, which have been detected in the environment [34]. A multi-analytical study [33] using high-resolution liquid chromatography, gas chromatography, and mass spectrometry identified 296 potential compounds, demonstrating that mass spectrometry methods offer more precise quantification, such as Pyro-GC-MS (pyrolysis coupled with gas chromatography–mass spectrometry) [32,38]. A recent study also highlighted the importance of identifying organic compounds leachable from complex rubber matrices, such as recycled rubber, where 46 sample-specific compounds were identified by GC/MS [39].

In Europe, the disposal of end-of-life tires (ELTs) has significantly shifted from landfills to recovery methods [40] to reduce the need for virgin materials [41] and repurpose them into various applications like playground flooring [42], artificial turf, concrete products [43], asphalt [44], beds for train lines, noise barriers, and outdoor tiles [41,45]. However, the literature presents mixed findings on the potential environmental and human health risks associated with these materials. While some studies indicate that ELTs are safe [45,46], others suggest potential hazards [41,47]. One study has revealed the presence of 306 chemicals in rubber particles released from EOL products, with 197 meeting carcinogenicity criteria [48]. Implementing science-based regulations and standardizing tire-derived products could improve their safety and acceptance, especially in sensitive applications involving vulnerable populations like children [41], since a recent study [49] of 10 playgrounds in Sydney highlighted the risk of serious skin burns in children due to the high surface temperatures of playground flooring in the sun, particularly wet pour rubber and synthetic turf.

In our previous research [50], we successfully immobilized titanium dioxide (TiO_2) on the surface of rubber tiles made from EOL tires and achieved photocatalytic decomposition. TiO_2 is of particular interest due to its numerous properties; including the photocatalytic decomposition of organic substances [51–53], which enhances surface self-cleaning [54–56], achieves an antibacterial effect [57–59], helps reduce photoaging through the absorption of ultraviolet light [60,61], and improves the mechanical properties of the material [59]. For this reason, we studied how the modification of existing rubber tiles by immobilizing TiO_2 using the sol–gel method would impact on the aging process under the UV irradiation of

the material, focusing on surface integrity, rubber particle wear release, and the consequent environmental impact of leachate release.

2. Experimental Section

2.1. Materials

The reference rubber tiles (RRTs) used in this work were produced from recycled waste tires obtained from Gumiimpex-GRP Ltd. (Varaždin, Croatia). The waste tires were mechanically ground into rubber granulates of sizes 0.0–0.5 mm, 0.5–2.0 mm, and 2.0–3.5 mm. The rubber tiles used in this paper measured 1000 × 1000 × 10 mm and were made using 9 kg of rubber granulate, 380 g of binder (polyurethane Stobicoll® R352.00, STOCKMEIER Urethanes, Cernay, France), and 5 g of catalyst (DABCO K 2097, Air Products, Allentown, Pennsylvania, SAD). These ingredients were mixed for 5 min with an industrial mixer, placed in a mold, and pressed at 120 °C for 4 min. After pressing, the rubber tiles were removed from the mold and allowed to cool. The rubber tiles consisted mainly of 20% granulates sized 0.5–2.0 mm and 80% granulates sized 2.0–3.5 mm.

The prepared rubber tiles were then modified to achieve photocatalytic properties according to the procedure described in a previously published paper [50]. The modification involved the sol–gel immobilization of the TiO_2 photocatalyst, resulting in the sol–gel tile (SGT). The first step was preparing the rubber tile by etching its surface with sodium hydroxide solution (NaOH, 1:10, *w*:*v*) to achieve a rougher surface and to form -OH groups [62]. Next, the sol–gel solution was prepared by mixing 2 g of TiO_2 (Evonik Industries AG, Essen, Germany, Aeroxid®, TiO_2 P25, 30 nm, 56 m^2/g, 75:25 anatase to rutile mas' ratio), 200 mL of deionized water, 200 mL ethanol (96%, GramMol, Zagreb, Croatia), 70 mL acetic acid (99–100% p.a., LabExpert, Split, Croatia), and 5 mL of tetraethyl orthosilicate (TEOS, ≥99.9% Sigma-Aldrich, St. Louis, MO, USA). This solution was stirred at 50 °C for 1 h. The rubber tile was then soaked in the solution for 10 min and dried at 80 °C for 20 min, four times in a row. At the end, the tile was left to dry for a week at room temperature.

2.2. Aging Test

The reference (RRTs) and modified rubber tiles (SGTs) were subjected to artificial accelerated aging in a solar simulator, the ISOSun (InfinityPV ApS, Jyllinge, Denmark). The chamber uses a 1200 W metal halide lamp as a UV source, which also heats the chamber. The temperature inside the chamber is controlled by a fan. The solar simulator generates bright white light that closely mimics the sun's spectrum, producing ozone and heat. Depending on the filter used, ISOSun can provide a good spectral match, with an intensity ranging from 0.5 to 1.5 solar equivalents, as well as widely used solar simulators with xenon lamps [63]. The spectral irradiance (standard filter) of the solar simulator (ISOSun) compared with the reference global horizontal irradiance spectrum (AM 1.5G) is shown in Figure 1. AM 1.5G is commonly used in terrestrial solar cell research, in accordance with the American Society for Testing and Materials (ASTM) G-173, as well as with the International Electrotechnical Commission IEC60904.

The samples were fixed in the chamber and exposed to UV irradiation for 28, 42, and 56 days, i.e., 4, 6, and 8 weeks. The correlation between accelerated aging time and real time for the material (rubber tiles) is calculated according to the following equation [64,65]:

$$\text{Accelerated Aging Time (AAT)} = \frac{\text{Desired Real Time (RT)}}{Q_{10}^{\left(\frac{T_{AA}-T_{RT}}{10}\right)}} \quad (1)$$

The accelerated aging temperature (T_{AA}) was maintained at 85 °C, while the ambient temperature (T_{RT}) was maintained at 19 °C. The ambient temperature aging factor (Q_{10}) typically ranges between 1.8 and 2.5, with 2.0 being the most common value. According to the given setup parameters, 56.5 days of accelerated aging time (AAT) correspond to 15 years of desired real time (RT) [64,65]. Consequently, 4 and 6 weeks correspond to

7.5- and 11-year-old rubber tiles, respectively. Therefore, six rubber tiles were studied, differing in time period (weeks; W); RRT4W, RRT6W, and RRT8W, and SGT4W, SGT6W, and SGT8W, respectively.

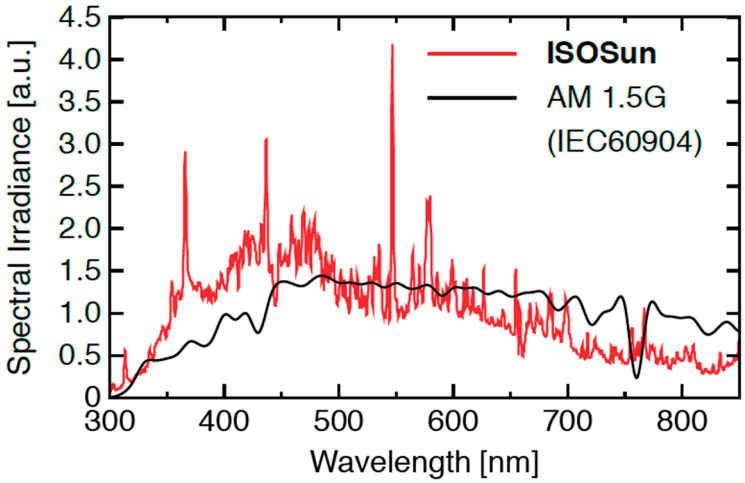

Figure 1. Representation of reference solar spectral irradiance (AM 1.5G—a global horizontal irradiance spectrum) compared with the one of the solar simulator (ISOSun) provided by the manufacturer.

2.3. Mechanical Properties—Abrasion Testing

The reference rubber tiles and TiO_2 sol–gel-coated rubber tiles were subjected to aging in the solar simulator (as described above). After undergoing the accelerated aging test, the mechanical properties in the form of abrasion were tested. The rubber wear test was performed using a Gibitre Abrasiometre A (Gibitre Instruments, Bergamo, Italy), which estimates the sample's resistance to abrasion according to the [66]. Abrasion was measured on a standard sample using a rotating drum equipped with standardized sandpaper, against which the specimen was pressed with a defined force until a rotating length of 40 m was achieved. Each sample was analyzed 3 times, and the results were expressed as the averages of these three measurements. The rubber particles collected after testing were characterized by FTIR and LC/MS QTOF analysis (as described below).

2.4. Characterization

2.4.1. FTIR Spectroscopy

The infrared spectra of the investigated materials were recorded using a Fourier transform infrared (FTIR) spectrometer (Bruker Vertex 70, Billerica, MA, USA) equipped with an attenuated total reflection (ATR) accessory with a diamond crystal. In total, 32 scans were collected for each measurement over the spectral range of 375–4000 cm^{-1} with a resolution of 2 cm^{-1}.

2.4.2. Carbonyl Index (C.I.)

As an indicator of degradation and chemical changes due to UV aging, the indices of carbon–oxygen bonds (C−O) and carbonyl group bonds (C=O) were monitored, and the carbonyl index (C.I.) was calculated. The C.I. was calculated by the ratio between the integrated band absorbance of the carbonyl (C=O) peak from 1850 to 1650 cm^{-1} and that of the methylene (CH_2) scissoring peak from 1500 to 1425 cm^{-1}, as expressed in the following equation [12,67]:

$$\text{C.I.}(\text{C}=\text{O}) = \frac{\text{area under band A}_{1850-1650\text{cm}^{-1}}}{\text{area under band A}_{1500-1425\text{cm}^{-1}}} \quad (2)$$

For the carbon–oxygen bonds, peaks from 1300 to 1140 cm^{-1} were considered and are expressed in the following equation [12,68]:

$$\text{C.I.}(\text{C}-0) = \frac{\text{area under band A}_{1300-1140\text{cm}^{-1}}}{\text{area under band A}_{1500-1425\text{cm}^{-1}}} \quad (3)$$

The area under the band was calculated using the peak analysis tool in the SpectraGryph 1.2 spectroscopy software options.

2.5. Water Leachate Testing (LC/MS QTOF)

Six samples were prepared for the water leachate test. The first four samples included reference rubber tiles (RRTs) before and after 8 weeks of artificial accelerated aging (RRT8W) and modified rubber tiles (SGTs) before and after 8 weeks of artificial accelerated aging (SGT8W). The last two samples were rubber particles (RRT8W-RP, SGT8W-RP) obtained via abrasion from the RRT8W and SGT8W. The masses of all 6 samples were weighed and placed in laboratory beakers, to which distilled water was added at the liquid-to-sample ratio (L:S) of 1:20, and were sealed with parafilm. The first four samples, consisting of whole substrates, were left to soak for 24 h, mimicking the static conditions of tiles placed in the environment, while the rubber particles obtained after surface abrasion were placed on a magnetic stirrer for 24 h, mimicking the dynamic conditions of particles in the environment. After 24 h, the samples were filtered (0.22 µm, PET, Chromafil, Macherey-Nagel, Düren, Germany) and prepared for high-resolution analysis by liquid chromatography coupled with quadrupole time-of-flight mass spectrometry (LC/MS QTOF, Agilent 6530 C Accurate Mass Q-TOF LC/MS with LC System Agilent 1260 Infinity II, Santa Clara, CA, USA). The samples were analyzed in accordance with the modified LC/MS method 5991-6627EN [69], created for acquiring the Agilent MassHunter Water Screening Personal Compound Database and Library (PCDL), which includes a list of more than 1400 environmental contaminants (Agilent Water Screening PCDL B.07.00 Water).

Chromatographic separation was performed on an Agilent Zorbax SB-Aq column (4.6 × 150 mm, 3.5 µm, Agilent Technologies, Santa Clara, CA, USA) at 40 °C with a 20 min run time and 5 min post time. Prior to each analysis, the column was conditioned and equilibrated with the intended solvent by running a sample method without sample injection. The flow rate was 0.40 mL/min with an injection volume of 5 mL. For the analysis, chemicals of LC/MS purity were used as follows: ultrapure water (LC/MS, VWR Chemicals BDH, Radnor, PA, USA), acetonitrile (LC/MS, Honeywell, Seelze, Germany), acetic acid (LC/MS, VWR Chemicals BDH, Radnor, PA, USA), and ammonium acetate (LC/MS, Carlo Erba Reagents, Milan, Lombardy, Italy). The mobile phase contained solvent A (MilliQ water with 0.1% acetic acid and 1 mM ammonium acetate ($v/v/v$)) and solvent B (0.1% acetic acid in acetonitrile). The first gradient mode started with a 2.00 min isocratic elution at 100% A, followed by a 12.00 min linear gradient and a 2.00 min isocratic elution with 2% A. Afterwards, the gradient was linearly returned to 100% A over 3.00 min and maintained until the end of the run time. The analyses were conducted in both positive and negative ion modes with collision energies set at 0, 10, and 40 V. The mass spectrometry parameters were as follows: drying gas temperature at 160 °C with a flow rate of 12 L/min; sheath gas temperature at 350 °C with a flow rate of 12 L/min; and a nebulizer pressure of 30 psi. The fragmentor voltage was set at 100 V, while the nozzle and capillary voltage were 1000 V and 3500 V in negative mode, and 500 V and 4500 V in positive mode, respectively. A summarized overview of the LC/MS QTOF method parameters is shown in Tables S1 and S2.

The obtained data were processed by using MassHunter Workstation Profinder Software B.10.00 in both positive and negative modes. A targeted-feature-extraction data mining algorithm was employed, and results with a sufficient score were further discussed (>85). In the positive mode, $[M+H]^+$ and $[M+NH_4]^+$ species were considered as charge carriers, while in the negative mode, $[M-H]^-$ and $[M+CH_3COO]^-$ species were considered, as these species are predominantly represented in the MS spectra included in the Water

Screening PCDL B.07.00 database. Furthermore, based on a literature review [34], common plasticizers were listed and analyzed by using MassHunter Workstation Qualitative Analysis Software B.10.00. Details can be found in the Supplementary Materials in Table S3 and Figures S1–S3. Compounds were identified based on these criteria.

3. Results and Discussion

3.1. FTIR Analysis

The photooxidative degradation of the studied rubber tiles was examined by FTIR to monitor changes in the structure of macromolecules. Figure 2 shows the FTIR spectra of the reference rubber tile before and after 4, 6, and 8 weeks of exposure to UV irradiation. Photooxidative decomposition resulted in the appearance of peaks at 1715 cm^{-1}, 1432 cm^{-1}, 1150 cm^{-1}, and 1080 cm^{-1}, attributed to newly formed chemical structures, namely ketones (C=O) and carbon–oxygen groups (C−O, O−C=O, C−O−O−) [12,70]. As observed in Figure 2, the increase in the intensity of the C=O bands is centered around 1715 cm^{-1} [12,68,70–72]. The absorption band at 1432 cm^{-1} is a characteristic of CH_2 formation [71]. Furthermore, the bands around 1085–1150 cm^{-1} can be attributed to C-O stretching [68,73]. As shown in Figure 2, the peaks are proportionally intensified with prolonged UV irradiation, which can be attributed to the initial stability of the rubber granulate and polyurethane.

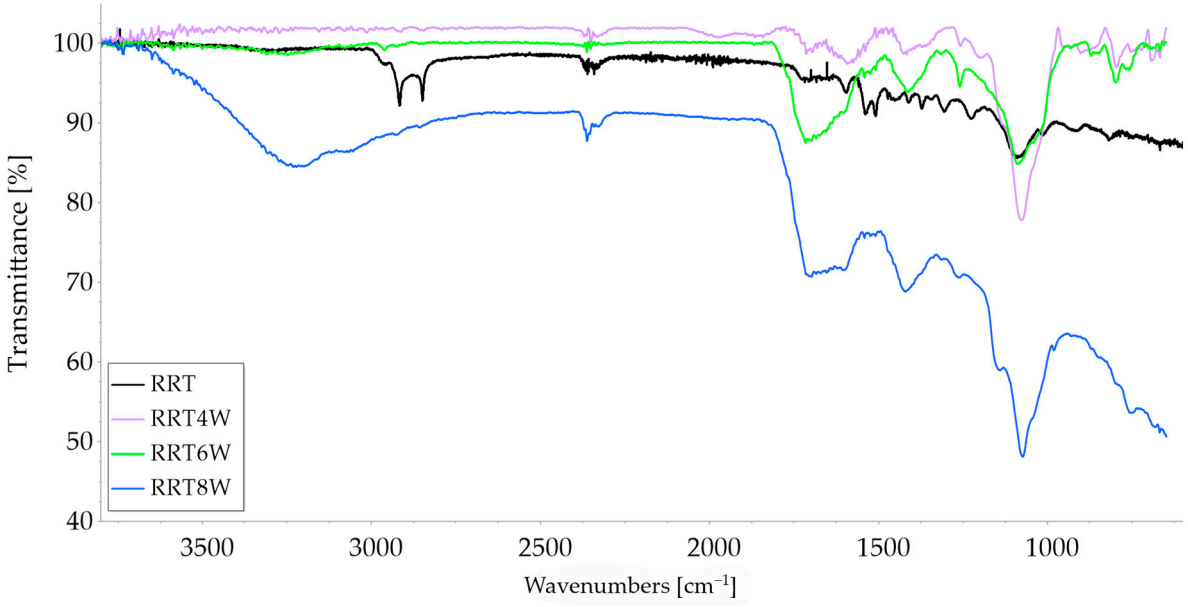

Figure 2. FTIR spectra of reference rubber tiles (RRTs) UV-irradiated for 4 (RRT4W), 6 (RRT6W), and 8 (RRT8W) weeks.

Figure 3 shows the FTIR spectra of both the reference and modified rubber tiles that were UV-irradiated for 8 weeks to compare the results.

It can be seen that the peak at RRT8W around 1715 cm^{-1} has increased, which may be associated with stronger photooxidative degradation in this sample [12,70,71]. Additionally, Figure 3 shows a broad peak, approximately between 3200–3500 cm^{-1}, which can be attributed to the presence of a hydroxyl group [15,68,71]. The RRT8W spectra show peaks at 1100 cm^{-1}, likely due to C−O stretching, and around 1400 cm^{-1}, which could be related to S=O stretching. In contrast, SGT8W has one peak stronger at 2390 cm^{-1}, potentially related to O=C=O stretching from carbon dioxide [74].

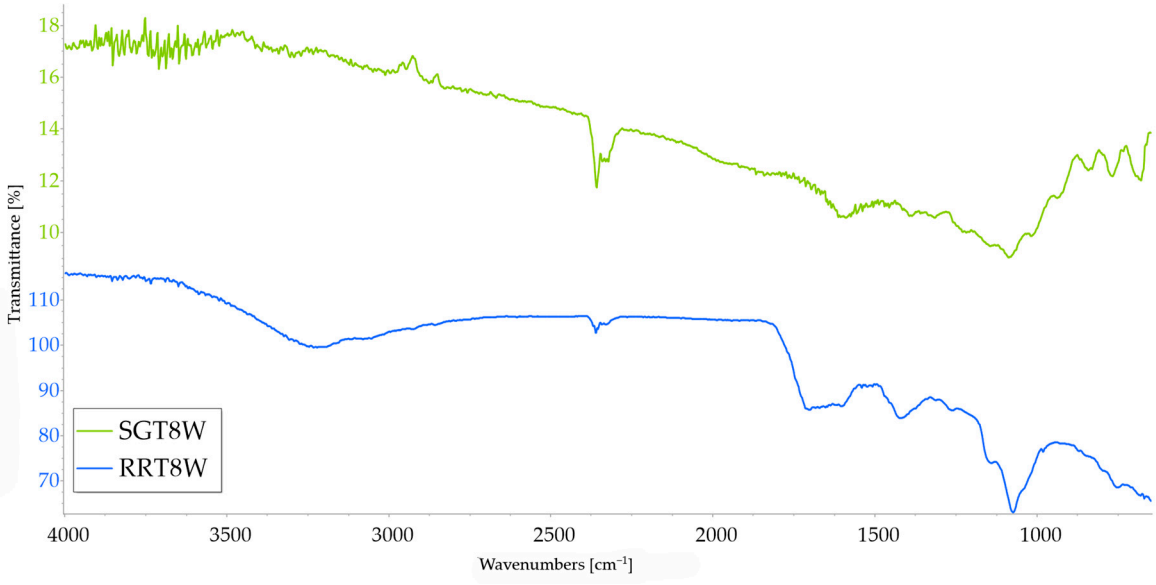

Figure 3. FTIR spectra of reference rubber tile (RRT8W) and modified rubber tile (SGT8W) UV-irradiated for 8 weeks.

3.2. Carbonyl Index (C.I.)

Table 1 lists the indices of the carbonyl index calculated for the C=O and C−O groups using the reference peaks in the range of 1500 to 1425 cm^{-1}, similarly as in the published literature [12,67]. In addition, the indices were determined for the upper (U) side (RRT/x/U; SGT/x/U) and the bottom (B) side (RRT/x/B; SGT/x/ B) of the rubber substrate exposed to UV irradiation to determine whether the UV irradiation had penetrated through the entire substrate [12]. Regarding the upper (U) side of the RRT and SGT substrates, the index calculated for the C=O group region showed an increase with UV aging, indicating the oxidation and degradation of the rubber material [12]. Initially, SGT/0 had a lower value (0.5410) compared to RRT/0 (0.6204). After 4 weeks, both substrates (RRT/4W/U and SGT/4W/U) exhibited an increase in the C=O index, followed by a trend in decreasing values at 6 weeks (RRT/6W/U and SGT/6W/U). Ultimately, SGT/8W/U showed a lower C=O index (0.8130) compared to RRT/8W/U (1.1850), suggesting that TiO_2 may effectively reduce the extent of oxidation and degradation in the UV-exposed upper part [75].

Table 1. Indicators of carbonyl (C=O, 1715 cm^{-1}) and carbon–oxygen groups (C−O, 1180, 1230 cm^{-1}) of initial and aged rubber samples.

Sample	C=O 1850–1650	C−O 1300–1140	Sample	C=O 1850–1650	C−O 1300–1140
RRT/0	0.6204	1.2262	SGT/0	0.5410	1.1561
RRT/4W/U	1.5639	7.3035	SGT/4W/U	0.8111	1.3107
RRT/6W/U	0.9748	4.2755	SGT/6W/U	0.7781	1.2532
RRT/8W/U	1.1850	0.8438	SGT/8W/U	0.8130	1.2663
RRT/4W/B	1.1167	2.3274	SGT/4W/B	0.7811	1.0137
RRT/6W/B	2.1125	1.3821	SGT/6W/B	0.7234	1.5315
RRT/8W/B	0.7485	1.2005	SGT/8W/B	0.8445	1.1907

As for the bottom (B) side of the substrates, after 4 weeks of irradiation, RRT/4W/B exhibited a twofold increase compared to SGT/4W/B. Subsequently, RRT/4W/B continued to show an upward trend, with RRT/6W/B increasing significantly to 2.1125. On the other hand, SGT/4W/B stagnated, and the value for SGT/6W/B was even lower (0.7234). After 8 weeks of irradiation, the value for RRT/8W/B decreased (0.7485), while SGT/8W/B had a final value of 0.8445.

The TiO_2 sol–gel coating effectively contributed to maintaining a lower carbonyl index for the C=O region throughout the irradiation period, as it was observed in [75]. Finally, SGT/8W/U showed significantly better results compared to RRT/8W/U. Although the value for SGT/8W/B was higher than that for RRT/8W/B, the SGTs maintained more consistent values throughout the entire irradiation period, with minimal fluctuations, as was the case with the RRTs.

A similar trend was observed for the C−O groups. Initially, the indices were approximately equal: RRT/0 = 1.2262, SGT/0 = 1.1561. However, after 4 weeks of irradiation, RRT/4W/U increased significantly to 7.3035, followed by a decreasing trend (RRT/6W/U = 4.2755, RRT/8W/U = 0.8438). On the other hand, the indices for SGT/4W/U, SGT/6W/U, and SGT/8W/U remained relatively stable without any drastic fluctuations. The value for SGT/8W/U was 1.2663, which is higher than RRT/8W/U, but the TiO_2 coating also contributed to maintaining lower indices during the entire irradiation period. Overall, the values for the C−O groups were approximately similar, with no major deviations observed.

Therefore, fluctuations in the RRT values confirm that the aging of polymer materials under the combined effects of light, heat, and oxygen is an autocatalytic process primarily driven by free radical reactions. When the energy from UV light exceeds the bond dissociation energy of the polymer molecules, it causes bond breakage and the formation of more reactive groups. This promotes the initiation of chain reactions, marking the first stage of aging. As the chain reactions progress, their transfer increases rapidly, significantly accelerating the aging process. On the other hand, TiO_2 can absorb and reflect UV irradiation, thereby inhibiting the initial stage of the aging chain reaction. This prevents the propagation and transfer of chains during the second stage, slowing down the overall aging process [75].

3.3. Mechanical Properties—Abrasion Testing

The abrasion results (Figure 4) indicate that for both samples (RRT and SGT), the values increase with the weeks of experimental accelerated aging testing. While the volume of the abraded particles increases linearly for the unmodified RRT (Figure 4a), it increases logarithmically for the modified SGT (Figure 4b). Initially, the mechanical stress causes a greater release of rubber particles from the SGT compared to the RRT due to the sol–gel immobilization process, which degrades the surface integrity of the reference rubber tiles. However, the results of the carbonyl indices indicate that TiO_2 coating stabilizes degradation processes under UV irradiation, slowing down the autocatalytic processes of polymer degradation [75]. Therefore, while TiO_2 coating stabilizes polymer degradation caused by UV irradiation on the main SGT compared to the RRT, the drawback of the sol–gel immobilization process is an increased release of particles. Consequently, the application of the SGT is limited to the area where less abrasion is expected, such as noise barrier tiles.

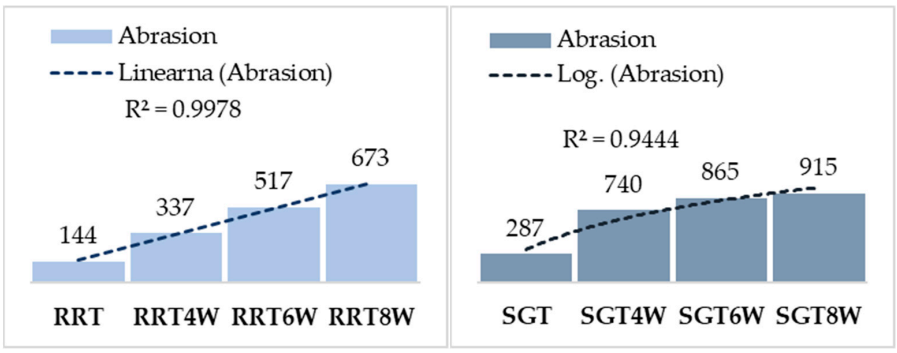

(**a**) (**b**)

Figure 4. Results of abrasion test expressed in mm^3: (**a**) unmodified RRT and (**b**) modified by sol–gel method rubber tiles (SGTs) over different periods (4, 6, and 8 weeks).

3.4. Water Lecheate Testing (LC/MS QTOF)

In the literature review [34,76], it was widely recognized that most chemicals of concern present in rubbers will eventually be found in tire wear particles, such as polycyclic aromatic hydrocarbons (PAHs), metals, volatile organic compounds (VOCs), plasticizers, antioxidants, and additives. Phthalates, a common class of compounds used in tire manufacturing, are widely utilized as plasticizers typically incorporated into rubber at concentrations below 30% by weight. The most commonly used phthalates are dibutyl phthalate, diethyl phthalate, di(2-ethylhexyl) phthalate [77], diisobutyl phthalate, and dimethyl phthalate. A recent study on tire and road wear microplastic (TRWMP) composition in China highlighted phthalates as being predominant in TRWMP release, accounting for 64.8% of release on average [78].

In this paper, three out of the stated five compounds were identified in water leachates (Figure 5). All three phthalates were also reported in rubber particles obtained above a football pitch and playground fabricated from crumb rubber [42,79]. As can be seen, a lower amount of diethyl phthalate and diisobutyl phthalate will be released into the environment when rubber tiles are coated with a TiO_2 layer. However, higher amounts will be released when it comes to dibutyl phthalate, most probably due to the impact of the immobilization process by the sol–gel method. Throughout the time and exposure of rubber tiles to UV irradiation, the TiO_2 coating on the SGT will contribute to less release dibutyl phthalate and diethyl phthalate. This is noteworthy, since dibutyl phthalate was detected in the air (17 ng/m^3) above the playgrounds where rubber tiles from secondary materials were placed [42].

Compound	CAS	Retention time	Peak area					
			RRT	RRT8W	RRT8W-RP	SGT	SGT8W	SGT8W-RP
Dibutyl phthalate	84-74-2	18.770±0.01	669071	2534617	DP	4401353	927814	DP
Diethyl phthalate	84-66-2	13.365±0.01	1396445	1115914	DP	780461	DP	DP
Diisobutyl phthalate	84-69-5	10.833±0.02	341909	116684	143181	325952	384916	523772

Figure 5. Identified phthalates (microplastics) in leachate samples (prior to and after accelerated aging tests) by LC/MS QTOF. DP stands for degradation product. The red color visually reflects the trend of the graph within the table.

Thus, as observed with the carbonyl indices, the TiO_2 coating generally contributes to the stabilization of and reduction in polymer degradation in the main SGT. However, when analyzing the release of specific compounds, the results indicate that a straightforward correlation cannot be established, as this relationship is influenced by several factors, including the chemical properties of the compounds, the rubber matrix, and environmental conditions. The same applies to the leaching of phthalates from rubber particles. Although abrasion tests indicated a higher release of particles from the SGT compared to the RRT (Figure 4), and a greater release of diisobutyl phthalate from rubber particles, the results for the other two phthalates suggest the degradation of the initial compounds, which requires further in-depth research.

Apart from phthalate release, a group of cyclic amines, benzothiazoles, benzotriazoles, alkylphenol ethoxylate, and derivatives are released into the environment from TWPs [34], but also from rubber tiles made from secondary raw materials [42]. Some benzothiazoles, such as *N*-cyclohexylbenzothiazole-2-sulfenamide (DCBS), dibenzothiazolyldisulfide (MBTS), and 2-(4-morpholinyl)-benzothiazole, are used as vulcanization accelerators in rubber production, and their transformation products have been frequently reported in the context of tires and road runoff, such as hydroxybenzothiazole (HOBT), mercaptobenzothiazole (MBT), and benzothiazole sulfonic acid (BTSA). However, not all of these compounds persist in the environment for long; they are either biodegraded (HOBT) or degraded via chemical reactions (such as MBT) [80]. In this study, benzotiazole, MBT, BTSA, and HOBT were identified after a database search (Table 2) as possible

compounds occurring in the leachate. Apart from HOBT, an additional two compounds with the same retention time were identified as possibly occurring: benzisothiazolinone and 2-mercaptobenzoxazole, also used in industrial applications for the vulcanization of rubber [39,81,82]. Apart from the plasticizers that were identified based on the literature review, plasticizers and solvents, dibutyl adipate, camphor, isoborneol, and acetamid were identified through a database search (Tables 2 and S4). These compounds are added to rubber to enhance flexibility and workability. Furthermore, the 4-nonylphenoxyacetic acid was identified as well. It is a degradation product of nonylphenol ethoxylates, used as surfactants and plasticizers [83]. Furthermore, additives, antioxidants, and corrosion inhibitors, such as 2-tert-butyl-4-methoxyphenol, methylsalicylate, 4-tert-octylphenol, and 4-hydroxybenzoic acid, were also identified in leachate (Table 2).

Table 2. List of identified compounds compiled using the Water Screening PCDL B.07.00 database (Agilent Technologies) with a matching score above 85.

Name	CAS	Mass	RT (min)	RSD (Mass, ppm)	Possible Origin
HOBT/2-Hydroxybenzothiazole	934-34-9	151.0101	14.617	1.59	rubber accelerator
BIT/Benzisothiazolinone	2634-33-5	151.0101	14.617	1.59	rubber and polymerized materials preservatives
2-Mercaptobenzoxazole	2382-96-9	151.0101	14.617	1.59	rubber accelerator
4-Nonylphenoxyacetic acid	3115-49-9	278.1885	17.605	1.57	Surfactant degradation
Benzothiazole-2-sulfonic acid	941-57-1	214.9721	12.509	2.52	rubber accelerator
4-Hydroxybenzoic acid		138.0326	12.576	2.58	Additive, corrosion inhibitor
Camphor		152.1205	17.122	1.46	Additive, plasticizer
Isoborneol	124-76-5	154.1359	16.247	5.03	Flavor and fragrance additive
Dibutyl adipate	105-99-7	258.1839	16.576	2.38	Plasticizers
Methylsalicylate	119-36-8	152.0484	13.839	1.45	UV light stabilizer
4-Methoxybenzoic acid	100-09-4	180.1156	17.132	5.6	Flavoring Agents
2-tert-Butyl-4-methoxyphenol	25013-16-5	192.1523	16.786	5.3	Antioxidant, additive
Ionone		256.0636	17.671	1.94	Flavoring agent
N4-Acetylsulfaguanidin (Acetamide)	19077-97-5	206.1682	18.594	5.27	solvent, plasticizer, stabilizer
4-tert-Octylphenol	140-66-9	125.9992	5.377	1.84	rubber additives, antioxidant
Ethyl sulfate	540-82-9	135.0155	12.801	1.44	Environmental contaminant
4-tert-Butylbenzoic acid	98-73-7	144.1147	16.283	2.86	Regulator of polymerization, inhibitor of corrosion
Benzothiazole		166.9865	15.414	1.56	rubber accelerator
MBT/2-Mercaptobenzothiazole	149-30-4	198.1414	17.767	4.38	Rubber accelerator

All these compounds are susceptible to further transformations. For instance, a recent study [84] investigated the environmental impact on air quality of rubber tiles derived from shredded EOL tires, which are commonly used in artificial turf and playgrounds. The researchers developed and validated an analytical method using ultrasound-assisted extraction and liquid chromatography-tandem mass spectrometry (UAE-LC/MS) to detect 11 hazardous compounds, including *N*-(1,3-dimethylbutyl)-*N*′-phenyl-p-phenylenediamine (6PPD), *N*,*N*′-diphenyl-p-phenylenediamine (DPPD), *N*-cyclohexylbenzothiazole-2-sulfenamide (CBS), 1,3-di-o-tolylguanidine (DTG), and hexamethoxymethylmelamine (HMMM). On the other hand, using high-resolution mass spectrometry (HRMS), out of 219 identified chemicals, 29 tire-related compounds, such as HMMM, 1,3-diphenylguanidine (DPG), dicyclohexy-

lurea (DCU), and *N*-cyclohexyl-2-benzothiazol-amine (DCMA), were detected in roadway runoff [85]. Photolysis experiments showed that compounds like DCU, DCMA, and DPG have low degradation rates, indicating their persistence in runoff. Consequently, the photocatalytic properties of TiO_2 can play a crucial role in reducing hazardous emissions and leachate into air and water by harnessing TiO_2's ability to degrade organic pollutants under UV light.

4. Conclusions

This study aimed to evaluate whether modifying existing rubber tiles made from waste tires with TiO_2 using the sol–gel method will affect the aging process under UV irradiation, with a focus on surface integrity, rubber particle wear, and the resulting environmental impact of leachate release.

The TiO_2 sol–gel coating contributed to maintaining a low C.I. for both the C=O and C-O regions throughout the irradiation period. The SGT/8W/U sample exhibited a significantly better C.I. for the C=O region compared to RRT/8W/U. As for the C-O region, although the C.I. for SGT/8W/U was 0.4255 higher than RRT/8W/U, the values for SGT/8W/U remained relatively stable and low throughout the irradiation period. The RRT/4W/U for the C-O region was 7.3035, which in real time would represent several years of exposure to such a high index. This is followed by RRT/6W/U, with an index of 4.2755. The sol–gel coating with TiO_2 led to stable and low indices, without large deviations, thereby inhibiting the initial stage of the aging chain reaction that was observed with the RRT.

Furthermore, this study found that rubber tiles coated with TiO_2 (SGTs) release lower amounts of diethyl phthalate and diisobutyl phthalate into the environment compared to uncoated tiles (RRTs). However, the release of dibutyl phthalate was higher, most probably due to the impact of the sol–gel immobilization process. Despite increased rubber tile wear and rubber particle release into the environment, the TiO_2 layer helps to reduce the release of dibutyl phthalate and diethyl phthalate from aged rubber tiles. However, the increased wear and release of rubber particles and the subsequent degradation of organic leachates require further in-depth research.

Additionally, aging may also affect the analytical assessment of microplastics (MPs) in environmental samples, which are likely to contain aged MPs. In contrast, many analytical methods are validated using pristine plastics, which may not accurately reflect the properties and behaviors of aged MPs [86]. This discrepancy underscores the need for further research to understand how aging influences the release and degradation of compounds, such as phthalates, from rubber materials, and their subsequent environmental and health impacts.

Supplementary Materials: The following supporting information can be downloaded at https://www.mdpi.com/article/10.3390/surfaces7030051/s1, Figure S1: Dibutyl phthalate—EIC (extracted ion chromatograph) at retention time 18.78 min; Figure S2: Diethyl phthalate—EIC (extracted ion chromatograph) at retention time 13.35 min; Figure S3: Diisobutyl phthalate—EIC (extracted ion chromatograph) at retention time 10.83 min; Table S1: LC (liquid chromatography) conditions; Table S2: MS (mass spectrometry) conditions; Table S3: Plasticizers reported in TWP [1]; Table S4: Detailed results—database search (combined table with graphical representation—showing compound abundance at given retention time).

Author Contributions: Conceptualization, P.B. and L.R.; methodology, P.B., L.R., I.P., and I.B.; software, P.B., L.R., I.B., and N.S.; validation, L.R., I.B., and I.G.; formal analysis, I.B.; investigation, P.B. and L.R.; resources, I.G.; data curation, P.B. and L.R.; writing—original draft preparation, P.B. and L.R.; writing—review and editing, P.B., L.R., I.P., N.S., and I.G.; visualization, P.B. and L.R.; supervision, L.R., I.B., and I.G.; project administration, I.G.; funding acquisition, I.G. All authors have read and agreed to the published version of the manuscript.

Funding: This work has been supported by the project "Recycling rubber & solar photocatalysis: ecological innovation for passive air and health protection", supported by the European Regional Development Fund, KK.01.1.1.07.0058.

Institutional Review Board Statement: Not applicable.

Informed Consent Statement: Not applicable.

Data Availability Statement: The original contributions presented in this study are included in the article/Supplementary Material, and further inquiries can be directed to the corresponding author, particularly inquiries regarding the raw data. The raw data will be made available by the authors on request.

Acknowledgments: This work was supported by the European union from European Regional Development Fund under the grant KK.01.1.1.04.0006 (OS-Mi project). The authors would also like to acknowledge the Gumiimpex Ltd. company as the partner on the stated project and for providing the materials. F. Menges "Spectragryph—optical spectroscopy software", Version 1.x.x, 202x, http://www.effemm2.de/spectragryph/, accessed on 13 May 2024.

Conflicts of Interest: The authors declare no conflicts of interest. The sponsors had no role in the design, execution, interpretation, or writing of this study.

References

1. ETRMA-European Tyre & Rubber Manufacturers' Association, (n.d.). Available online: https://www.etrma.org/ (accessed on 29 March 2024).
2. Valentini, F.; Pegoretti, A. End-of-life options of tyres. A review. *Adv. Ind. Eng. Polym. Res.* **2022**, *5*, 203–213. [CrossRef]
3. Armada, D.; Llompart, M.; Celeiro, M.; Garcia-WCastro, P.; Ratola, N.; Dagnac, T.; de Boer, J. Global evaluation of the chemical hazard of recycled tire crumb rubber employed on worldwide synthetic turf football pitches. *Sci. Total Environ.* **2022**, *812*, 152542. [CrossRef] [PubMed]
4. Martin's Rubber Company. (n.d.). Available online: https://www.martins-rubber.co.uk/ (accessed on 29 March 2024).
5. Itoh, Y.; Gu, H. Effect of Ultraviolet Irradiation on Surface Rubber Used in Bridge Bearings. *J. Struct. Eng.* **2007**, *53*, 696–705.
6. Iwase, Y.; Shindo, T.; Kondo, H.; Ohtake, Y.; Kawahara, S. Ozone degradation of vulcanized isoprene rubber as a function of humidity. *Polym. Degrad. Stab.* **2017**, *142*, 209–216. [CrossRef]
7. Pourebrahimi, S.; Pirooz, M. Microplastic pollution in the marine environment: A review. *J. Hazard. Mater. Adv.* **2023**, *10*, 100327. [CrossRef]
8. Kye, H.; Kim, J.; Ju, S.; Lee, J.; Lim, C.; Yoon, Y. Microplastics in water systems: A review of their impacts on the environment and their potential hazards. *Heliyon* **2023**, *9*, e14359. [CrossRef]
9. Zhai, X.; Zheng, H.; Xu, Y.; Zhao, R.; Wang, W.; Guo, H. Characterization and quantification of microplastics in indoor environments. *Heliyon* **2023**, *9*, e15901. [CrossRef]
10. Sutkar, P.R.; Gadewar, R.D.; Dhulap, V.P. Recent trends in degradation of microplastics in the environment: A state-of-the-art review. *J. Hazard. Mater. Adv.* **2023**, *11*, 100343. [CrossRef]
11. Rasmussen, L.A.; Lykkemark, J.; Andersen, T.R.; Vollertsen, J. Permeable pavements: A possible sink for tyre wear particles and other microplastics? *Sci. Total Environ.* **2023**, *869*, 161770. [CrossRef]
12. Zjačić, J.P.; Vujasinović, M.; Kovačić, M.; Božić, A.L.; Kušić, H.; Katančić, Z.; Hrnjak-Murgić, Z. From Macro to Micro Plastics; Influence of Photo-oxidative Degradation. *Kem. Ind.* **2023**, *72*, 463–471. [CrossRef]
13. Enfrin, M.; Myszka, R.; Giustozzi, F. Paving roads with recycled plastics: Microplastic pollution or eco-friendly solution? *J. Hazard. Mater.* **2022**, *437*, 129334. [CrossRef]
14. Österlund, H.; Blecken, G.; Lange, K.; Marsalek, J.; Gopinath, K.; Viklander, M. Microplastics in urban catchments: Review of sources, pathways, and entry into stormwater. *Sci. Total Environ.* **2023**, *858*, 159781. [CrossRef] [PubMed]
15. Klun, B.; Rozman, U.; Kalčíková, G. Environmental aging and biodegradation of tire wear microplastics in the aquatic environment. *J. Environ. Chem. Eng.* **2023**, *11*, 110604. [CrossRef]
16. Prasittisopin, L.; Ferdous, W.; Kamchoom, V. Microplastics in construction and built environment. *Dev. Built Environ.* **2023**, *15*, 100188. [CrossRef]
17. An, L.; Liu, Q.; Deng, Y.; Wu, W.; Gao, Y.; Ling, W. Sources of Microplastic in the Environment. *Handb. Environ. Chem.* **2020**, *95*, 143–159. [CrossRef]
18. Chae, E.; Yang, S.R.; Choi, S.S. Test method for abrasion behavior of tire tread compounds using the wear particles. *Polym. Test.* **2022**, *115*, 107758. [CrossRef]
19. Järlskog, I.; Jaramillo-Vogel, D.; Rausch, J.; Gustafsson, M.; Strömvall, A.M.; Andersson-Sköld, Y. Concentrations of tire wear microplastics and other traffic-derived non-exhaust particles in the road environment. *Environ. Int.* **2022**, *170*, 107618. [CrossRef]
20. Kovochich, M.; Oh, S.C.; Lee, J.P.; Parker, J.A.; Barber, T.; Unice, K. Characterization of tire and road wear particles in urban river samples. *Environ. Adv.* **2023**, *12*, 100385. [CrossRef]

21. Rausch, J.; Jaramillo-Vogel, D.; Perseguers, S.; Schnidrig, N.; Grobéty, B.; Yajan, P. Automated identification and quantification of tire wear particles (TWP) in airborne dust: SEM/EDX single particle analysis coupled to a machine learning classifier. *Sci. Total Environ.* **2022**, *803*, 149832. [CrossRef]
22. Halle, L.L.; Palmqvist, A.; Kampmann, K.; Khan, F.R. Ecotoxicology of micronized tire rubber: Past, present and future considerations. *Sci. Total Environ.* **2020**, *706*, 135694. [CrossRef]
23. Wagner, S.; Hüffer, T.; Klöckner, P.; Wehrhahn, M.; Hofmann, T.; Reemtsma, T. Tire wear particles in the aquatic environment—A review on generation, analysis, occurrence, fate and effects. *Water Res.* **2018**, *139*, 83–100. [CrossRef] [PubMed]
24. Järlskog, I.; Strömvall, A.M.; Magnusson, K.; Gustafsson, M.; Polukarova, M.; Galfi, H.; Aronsson, M.; Andersson-Sköld, Y. Occurrence of tire and bitumen wear microplastics on urban streets and in sweepsand and washwater. *Sci. Total Environ.* **2020**, *729*, 138950. [CrossRef] [PubMed]
25. Goßmann, I.; Halbach, M.; Scholz-Böttcher, B.M. Car and truck tire wear particles in complex environmental samples—A quantitative comparison with "traditional" microplastic polymer mass loads. *Sci. Total Environ.* **2021**, *773*, 145667. [CrossRef] [PubMed]
26. Ferreira, T.; Homem, V.; Cereceda-Balic, F.; Fadic, X.; Alves, A.; Ratola, N. Are volatile methylsiloxanes in downcycled tire microplastics? Levels and human exposure estimation in synthetic turf football fields. *Environ. Sci. Pollut. Res.* **2024**, *31*, 11950–11967. [CrossRef]
27. Hartmann, N.B.; Hüffer, T.; Thompson, R.C.; Hassellöv, M.; Verschoor, A.; Daugaard, A.E.; Rist, S.; Karlsson, T.; Brennholt, N.; Cole, M.; et al. Are We Speaking the Same Language? Recommendations for a Definition and Categorization Framework for Plastic Debris. *Environ. Sci. Technol.* **2019**, *53*, 1039–1047. [CrossRef] [PubMed]
28. Jan Kole, P.; Löhr, A.J.; Van Belleghem, F.G.A.J.; Ragas, A.M.J. Wear and tear of tyres: A stealthy source of microplastics in the environment. *Int. J. Environ. Res. Public Health* **2017**, *14*, 1265. [CrossRef]
29. Rødland, E.S.; Gustafsson, M.; Jaramillo-Vogel, D.; Järlskog, I.; Müller, K.; Rauert, C.; Rausch, J.; Wagner, S. Analytical challenges and possibilities for the quantification of tire-road wear particles. *TrAC Trends Anal. Chem.* **2023**, *165*, 117121. [CrossRef]
30. Baensch-Baltruschat, B.; Kocher, B.; Stock, F.; Reifferscheid, G. Tyre and road wear particles (TRWP)—A review of generation, properties, emissions, human health risk, ecotoxicity, and fate in the environment. *Sci. Total Environ.* **2020**, *733*, 137823. [CrossRef]
31. Baensch-Baltruschat, B.; Kocher, B.; Kochleus, C.; Stock, F.; Reifferscheid, G. Tyre and road wear particles—A calculation of generation, transport and release to water and soil with special regard to German roads. *Sci. Total Environ.* **2021**, *752*, 141939. [CrossRef]
32. Rødland, E.S.; Lind, O.C.; Reid, M.J.; Heier, L.S.; Okoffo, E.D.; Rauert, C.; Thomas, K.V.; Meland, S. Occurrence of tire and road wear particles in urban and peri-urban snowbanks, and their potential environmental implications. *Sci. Total Environ.* **2022**, *824*, 153785. [CrossRef]
33. Calarnou, L.; Traïkia, M.; Leremboure, M.; Malosse, L.; Dronet, S.; Delort, A.-M.; Besse-Hoggan, P.; Eyheraguibel, B. Assessing biodegradation of roadway particles via complementary mass spectrometry and NMR analyses. *Sci. Total Environ.* **2023**, *900*, 165698. [CrossRef] [PubMed]
34. Johannessen, C.; Liggio, J.; Zhang, X.; Saini, A.; Harner, T. Composition and transformation chemistry of tire-wear derived organic chemicals and implications for air pollution. *Atmos. Pollut. Res.* **2022**, *13*, 101533. [CrossRef]
35. Knight, L.J.; Parker-Jurd, F.N.F.; Al-Sid-Cheikh, M.; Thompson, R.C. Tyre wear particles: An abundant yet widely unreported microplastic? *Environ. Sci. Pollut. Res.* **2020**, *27*, 18345–18354. [CrossRef] [PubMed]
36. Giechaskiel, B.; Grigoratos, T.; Mathissen, M.; Quik, J.; Tromp, P.; Gustafsson, M.; Franco, V.; Dilara, P. Contribution of Road Vehicle Tyre Wear to Microplastics and Ambient Air Pollution. *Sustainability* **2024**, *16*, 522. [CrossRef]
37. Rauert, C.; Rødland, E.S.; Okoffo, E.D.; Reid, M.J.; Meland, S.; Thomas, K.V. Challenges with Quantifying Tire Road Wear Particles: Recognizing the Need for Further Refinement of the ISO Technical Specification. *Environ. Sci. Technol. Lett.* **2021**, *8*, 231–236. [CrossRef]
38. Rosso, B.; Gregoris, E.; Litti, L.; Zorzi, F.; Fiorini, M.; Bravo, B.; Barbante, C.; Gambaro, A.; Corami, F. Identification and quantification of tire wear particles by employing different cross-validation techniques: FTIR-ATR Micro-FTIR, Pyr-GC/MS, and SEM. *Environ. Pollut.* **2023**, *326*, 121511. [CrossRef]
39. Skoczyńska, E.; Leonards, P.E.G.; Llompart, M.; de Boer, J. Analysis of recycled rubber: Development of an analytical method and determination of polycyclic aromatic hydrocarbons and heterocyclic aromatic compounds in rubber matrices. *Chemosphere* **2021**, *276*, 130076. [CrossRef]
40. Ciccu, R.; Costa, G. Recycling of secondary raw materials from end-of-life car tires. *WIT Trans. Ecol. Environ.* **2012**, *155*, 1115–1126. [CrossRef]
41. Patricio, J.; Andersson-Sköld, Y.; Gustafsson, M. End-of-Life Tyres Applications—Technologies and Environmental Impacts. 2021. Available online: https://www.diva-portal.org/smash/record.jsf?pid=diva2:1611409&dswid=9797 (accessed on 17 March 2024).
42. Armada, D.; Celeiro, M.; Dagnac, T.; Llompart, M. Green methodology based on active air sampling followed by solid phase microextraction and gas chromatography-tandem mass spectrometry analysis to determine hazardous substances in different environments related to tire rubber. *J. Chromatogr. A* **2022**, *1668*, 462911. [CrossRef]
43. Grynkiewicz-Bylina, B.; Słomka-Słupik, B.; Rakwic, B. Tests of Cement and Slag Mortars with SBR Rubber Granulates in Terms of Ecotoxicity and Strength. *Inżynieria Miner.* **2024**, *2*, 153–162. [CrossRef]
44. Yu, H.; Bai, X.; Qian, G.; Wei, H.; Gong, X.; Jin, J.; Li, Z. Impact of Ultraviolet Radiation on the Aging Properties of SBS-Modified Asphalt Binders. *Polymers* **2019**, *11*, 1111. [CrossRef]

45. Bokkers, B.G.H.; Guichelaar, S.K.; Bakker, M.I. Assessment of the Product Limit for PAHs in Rubber Articles. The Case of Shock-Absorbing Tiles. 2016. Available online: https://www.rivm.nl/bibliotheek/rapporten/2016-0184.html (accessed on 29 April 2024).
46. Pronk, M.E.J.; Woutersen, M.; Herremans, J.M.M. Synthetic turf pitches with rubber granulate infill: Are there health risks for people playing sports on such pitches? *J. Expo. Sci. Environ. Epidemiol.* **2020**, *30*, 567–584. [CrossRef] [PubMed]
47. Celeiro, M.; Armada, D.; Ratola, N.; Dagnac, T.; de Boer, J.; Llompart, M. Evaluation of chemicals of environmental concern in crumb rubber and water leachates from several types of synthetic turf football pitches. *Chemosphere* **2021**, *270*, 128610. [CrossRef] [PubMed]
48. Perkins, A.N.; Inayat-Hussain, S.H.; Deziel, N.C.; Johnson, C.H.; Ferguson, S.S.; Garcia-Milian, R.; Thompson, D.C.; Vasiliou, V. Evaluation of potential carcinogenicity of organic chemicals in synthetic turf crumb rubber. *Environ. Res.* **2019**, *169*, 163–172. [CrossRef] [PubMed]
49. Pfautsch, S.; Wujeska-Klause, A.; Walters, J. Outdoor playgrounds and climate change: Importance of surface materials and shade to extend play time and prevent burn injuries. *Build. Environ.* **2022**, *223*, 109500. [CrossRef]
50. Benjak, P.; Radetić, L.; Tomaš, M.; Brnardić, I.; Radetić, B.; Špada, V.; Grčić, I. Rubber Tiles Made from Secondary Raw Materials with Immobilized Titanium Dioxide as Passive Air Protection. *Processes* **2023**, *11*, 125. [CrossRef]
51. Leng, Z.; Yu, H. Novel Method of Coating Titanium Dioxide on to Asphalt Mixture Based on the Breath Figure Process for Air-Purifying Purpose. *J. Mater. Civ. Eng.* **2016**, *28*, 04015188. [CrossRef]
52. Boonen, E.; Beeldens, A. Recent photocatalytic applications for air purification in Belgium. *Coatings* **2014**, *4*, 553–573. [CrossRef]
53. La Russa, M.F.; Rovella, N.; De Buergo, M.A.; Belfiore, C.M.; Pezzino, A.; Crisci, G.M.; Ruffolo, S.A. Nano-TiO_2 coatings for cultural heritage protection: The role of the binder on hydrophobic and self-cleaning efficacy. *Prog. Org. Coatings* **2016**, *91*, 1–8. [CrossRef]
54. Gherardi, F.; Maravelaki, P.N. Advances in the application of nanomaterials for natural stone conservation. *RILEM Tech. Lett.* **2022**, *7*, 20–29. [CrossRef]
55. Ruffolo, S.A.; Francesco, M.; Russa, L. Nanostructured Coatings for Stone Protection: An Overview. *Front. Mater.* **2019**, *6*, 147. [CrossRef]
56. Esposito, C.; Ingrosso, C.; Petronella, F.; Comparelli, R.; Striccoli, M.; Agostiano, A.; Frigione, M.; Curri, M.L. Progress in Organic Coatings A designed UV—Vis light curable coating nanocomposite based on colloidal TiO_2 NRs in a hybrid resin for stone protection. *Prog. Org. Coatings* **2018**, *122*, 290–301. [CrossRef]
57. Nazir, M.; Irfan, M.; Ali, I.; Abdul, M. Photonics and Nanostructures—Fundamentals and Applications Revealing antimicrobial and contrasting photocatalytic behavior of metal chalcogenide deposited P25-TiO_2 nanoparticles. *Photonics Nanostruct. Fundam. Appl.* **2019**, *36*, 100721. [CrossRef]
58. Dds, A.S.; Bahador, A.; Khalil, S.; Saffar, A.; Dds, S.; Zaman, M. The effect of TiO_2 and SiO_2 nanoparticles on flexural strength of poly (methyl methacrylate) acrylic resins. *J. Prosthodont. Res.* **2013**, *57*, 15–19. [CrossRef]
59. Salama, A.; Kamel, B.M.; Osman, T.A.; Rashad, R.M. Investigation of mechanical properties of UHMWPE composites reinforced with HAP þ TiO_2 fabricated by solvent dispersing technique. *J. Mater. Res. Technol.* **2022**, *21*, 4330–4343. [CrossRef]
60. Wang, L.; Liu, Q.; Jing, D.; Zhou, S.; Shao, L. ScienceDirect Biomechanical properties of nano-TiO_2 addition to a medical silicone elastomer: The effect of artificial ageing. *J. Dent.* **2014**, *42*, 475–483. [CrossRef]
61. Elsaka, S.E.; Hamouda, I.M.; Swain, M.V. Titanium dioxide nanoparticles addition to a conventional glass-ionomer restorative: Influence on physical and antibacterial properties. *J. Dent.* **2011**, *39*, 589–598. [CrossRef]
62. Nuzaimah, M.; Sapuan, S.M.; Nadlene, R.; Jawaid, M. Sodium hydroxide treatment ofwaste rubber crumb and its effects on properties of unsaturated polyester composites. *Appl. Sci.* **2020**, *10*, 3913. [CrossRef]
63. Tawfik, M.; Tonnellier, X.; Sansom, C. Light source selection for a solar simulator for thermal applications: A review. *Renew. Sustain. Energy Rev.* **2018**, *90*, 802–813. [CrossRef]
64. Krug, N.; Zarges, J.-C.; Heim, H.-P. Influence of ethylene oxide and gamma irradiation sterilization processes on the degradation behaviour of poly(lactic acid) (PLA) in the course of artificially accelerated aging. *Polym. Test.* **2024**, *132*, 108362. [CrossRef]
65. Lamberti, M.; Maurel-Pantel, A.; Lebon, F. Experimental and numerical evaluation of hydro-thermal ageing's effects on adhesive connections in offshore structures. *Ocean Eng.* **2023**, *290*, 116303. [CrossRef]
66. *ISO 4649:2024*; Rubber, Vulcanized or Thermoplastic—Determination of Abrasion Resistance Using a Rotating Cylindrical Drum Device. International Organization for Standardization (ISO): Geneva, Switzerland, 2024.
67. Almond, J.; Sugumaar, P.; Wenzel, M.N.; Hill, G.; Wallis, C. Determination of the carbonyl index of polyethylene and polypropylene using speci fi ed area under band methodology with ATR-FTIR Spectroscopy. *e-Polymers* **2020**, *20*, 369–381. [CrossRef]
68. Brandon, J.; Goldstein, M.; Ohman, M.D. Long-term aging and degradation of microplastic particles: Comparing in situ oceanic and experimental weathering patterns. *Mar. Pollut. Bull.* **2016**, *110*, 299–308. [CrossRef] [PubMed]
69. Berset, J.D.; Rennie, E.; Glauner, T. Screening and Identification of Emerging Contaminants in Wastewater Treatment Plant Effluents Using UHPLC/Q-TOF MS and an Accurate Mass Database and Library. 2016. Available online: https://sem.com.tr/wp-content/uploads/Screening-and-Identification-of-Emerging-Contaminants-in-Wastewater-Treatment-Plant.pdf (accessed on 17 September 2024).

70. Redon, A.; Le Cam, J.B.; Robin, E.; Miroir, M.; Fralin, J.C. Aging characterization of different nitrile butadiene rubbers for sealing in a pneumatic system: Linking the change of the physicochemical state to the mechanical properties. *J. Appl. Polym. Sci.* **2023**, *140*, e54068. [CrossRef]
71. Aielo, P.B.; Borges, F.A.; Romeira, K.M.; Miranda, M.C.R.; Arruda, L.B.D.; Paulo, P.N.; Drago, B.D.C.; Herculano, R.D. Evaluation of sodium diclofenac release using natural rubber latex as carrier. *Mater. Res.* **2014**, *17*, 146–152. [CrossRef]
72. Ling, L.; Li, J.; Zhang, G.; Sun, R.; Wong, C.P. Self-Healing and Shape Memory Linear Polyurethane Based on Disulfide Linkages with Excellent Mechanical Property. *Macromol. Res.* **2018**, *26*, 365–373. [CrossRef]
73. InstaNANO, FTIR Functional Group Database Table with Search-InstaNANO, (n.d.). Available online: https://instanano.com/ (accessed on 2 May 2024).
74. Merck, IR Spectrum Table by Frequency Range. (n.d.). Available online: https://www.sigmaaldrich.com/HR/en (accessed on 2 May 2024).
75. Liao, M.; Liu, Z.; Gao, Y.; Liu, L.; Xiang, S. Study on UV aging resistance of nano-TiO_2/montmorillonite/styrene-butadiene rubber composite modified asphalt based on rheological and microscopic properties. *Constr. Build. Mater.* **2021**, *301*, 124108. [CrossRef]
76. Gomes, F.O.; Rocha, M.R.; Alves, A.; Ratola, N. A review of potentially harmful chemicals in crumb rubber used in synthetic football pitches. *J. Hazard. Mater.* **2021**, *409*, 124998. [CrossRef]
77. Paredes, M.; Viteri, R.; Castillo, T.; Caminos, C.; Enyoh, C.E. Microplastics from degradation of tires in sewer networks of the city of Riobamba, Ecuador. *Environ. Eng. Res.* **2020**, *26*, 200276. [CrossRef]
78. Liu, M.; Xu, H.; Feng, R.; Gu, Y.; Bai, Y.; Zhang, N.; Wang, Q.; Ho, S.S.H.; Qu, L.; Shen, Z.; et al. Chemical composition and potential health risks of tire and road wear microplastics from light-duty vehicles in an urban tunnel in China. *Environ. Pollut.* **2023**, *330*, 121835. [CrossRef]
79. Celeiro, M.; Dagnac, T.; Llompart, M. Determination of priority and other hazardous substances in football fields of synthetic turf by gas chromatography-mass spectrometry: A health and environmental concern. *Chemosphere* **2018**, *195*, 201–211. [CrossRef] [PubMed]
80. Seiwert, B.; Klöckner, P.; Wagner, S.; Reemtsma, T. Source-related smart suspect screening in the aqueous environment: Search for tire-derived persistent and mobile trace organic contaminants in surface waters. *Anal. Bioanal. Chem.* **2020**, *412*, 4909–4919. [CrossRef] [PubMed]
81. National Center for Biotechnology Information, Compound Summary for CID 13625, 2(3H)-Benzothiazolone, PubChem. 2024. Available online: https://pubchem.ncbi.nlm.nih.gov/compound/13625 (accessed on 28 June 2024).
82. National Center for Biotechnology Information, PubChem Compound Summary for CID 17520, 1,2-Benzisothiazol-3(2H)-one, PubChem. 2024. Available online: https://pubchem.ncbi.nlm.nih.gov/compound/1_2-Benzisothiazol-3_2H_-one (accessed on 28 June 2024).
83. Vazquet-Duhalt, R.; Marquez-Rocha, F.; Ponce, E.; Licea, A.F.; Viana, M.T. Nonylphenol, an integrated vision of a pollutant. Scientific review. *Appl. Ecol. Environ. Res.* **2005**, *4*, 1–25. [CrossRef]
84. Duque-Villaverde, A.; Armada, D.; Dagnac, T.; Llompart, M. Recycled tire rubber materials in the spotlight. Determination of hazardous and lethal substances. *Sci. Total Environ.* **2024**, *929*, 172674. [CrossRef] [PubMed]
85. Chen, J.; Tang, T.; Li, Y.; Wang, R.; Chen, X.; Song, D.; Du, X.; Tao, X.; Zhou, J.; Dang, Z.; et al. Non-targeted screening and photolysis transformation of tire-related compounds in roadway runoff. *Sci. Total Environ.* **2024**, *924*, 171622. [CrossRef]
86. Binda, G.; Kalčíková, G.; Allan, I.J.; Hurley, R.; Rødland, E.; Spanu, D.; Nizzetto, L. Microplastic aging processes: Environmental relevance and analytical implications. *TrAC Trends Anal. Chem.* **2024**, *172*, 117566. [CrossRef]